Supporting Information

Solvent-Controlled Charge Storage Mechanisms of Spinel Oxide Electrodes in Mg Organohaloaluminate Electrolytes

Lu Wang,[†] Zhaohui Wang,[†,‡] Per Erik Vullum,[‡,§] Sverre M. Selbach,[†] Ann Mari Svensson,[†] and Fride Vullum-Bruer*[,†]

[†]Department of Materials Science and Engineering, Norwegian University of Science and Technology, NO-7491 Trondheim, Norway

[‡]SINTEF Materials and Chemistry, NO-7465 Trondheim, Norway

[§]Department of Physics, Norwegian University of Science and Technology, NO-7491 Trondheim, Norway

*Corresponding Authors. E-mail: fride.vullum-bruer@ntnu.no

EXPERIMENTAL SECTION

Energetics of the interaction between Mg cations and Mn_3O_4 host. DFT calculations were performed with the Vienna Ab initio Simulation Package (VASP).[1-5] The total energies were calculated by using PBEsol exchange-correlation fuctional.[6] The projector augmented wave (PAW) method[7] was used with the Mg_pv ($2s^2 2p^6$), Mn_pv ($3p^6$, $3d^5$, $4s^2$), O ($2s^2$, $2p^4$) and Li ($2s^1$) potentials supplied with VASP. Electron wave functions were expanded in plane waves up to a cut-off energy of 550 eV and the SCF convergence energy was set to 10^{-7} eV. The tetrahedron method with Blöchl correction was used for the electronic energy level occupancy. Brillouin zone integration was done with a 7×7×5 Γ-centered k-point mesh for the Mn_3O_4, $MgMn_3O_4$ and $LiMn_2O_4$ unit cells, with a similar k-point density for supercells. A Hubbard U of U = 4 eV was applied to Mn 3d state to correct self-interaction errors.[8] (The calculated magnetic moments of Mn^{2+} and Mn^{3+} were 4.5 μ_B and 3.4 μ_B, respectively.)

Geometry optimization was done by full relaxation of the structure until the Hellmann-Feynman forces on the ions were smaller than 10^{-3} eV $Å^{-1}$. For the defect structures, the ions were allowed to relax while keeping the lattice vectors fixed. Transition state searches were done with a 2×1×1 supercell using the climbing-image nudged elastic band (cNEB)[9] method as implemented in VASP. In the cNEB calculations, nine images were initialized by linear interpolation between the relaxed initial and final states. For all images along the band, atomic positions were relaxed until the Hellmann-Feynman forces on the ions converged to below 0.05 eV $Å^{-1}$ with fixed lattice vectors. Due to convergence issues, a Hubbard U was not used in cNEB calculations.[10] Only the nearest neighbor ions to the migrating Li or Mg were allowed to relax during cNEB calculations.

Preparation of APC electrolytes. In accordance with the procedure proposed by Aurbach *et al.*,[11] the APC-THF (tetrahydrofuran, Aldrich, anhydrous) electrolyte was prepared by the intensive mixing of the PhMgCl-THF solution (PhMgCl in THF, Aldrich, 99%) and the $AlCl_3$ ($AlCl_3$, Aldrich, 99.999%)-THF solution with a molar ratio of 2:1 under stirring for one day. The electrolyte preparation was performed in an Ar-filled glove box (<0.1 ppm of water and oxygen) and the concentration of the electrolyte was 0.4 mol L^{-1}.

The APC-G4 (tetraglyme, Aldrich, 99+%) electrolyte and the APC-DME (1,2-dimethoxyethane, Alfa Aesar, 99+%) electrolyte were obtained by first placing the synthesized APC-THF electrolyte under vacuum at room temperature overnight to fully evaporate the THF solvent. Then, introducing the necessary amount of G4 solvent or DME solvent into the obtained white precipitate and stirring overnight.

Material Characterization. The magnesiated Mn_3O_4 nanoparticles in APC electrolytes were characterized by a double Cs corrected coldFEG JEOL ARM200CF, operated at 200 kV and equipped with a large solid angle (0.98 srad) Centurio EDS detector and a Quantum ER GIF for EELS. Spectroscopy was performed in scanning transmission electron microscopy (STEM) mode. EDS and dual EELS maps were always acquired simultaneously. For the core loss EEL spectra (O K and Mn $L_{2,3}$ peaks) the low loss spectra, that included the zero loss peak, were used to calibrate the energy scale in every pixel of the map.

Electrochemical Measurements. Mn_3O_4 nanoparticles have been synthesized according to a procedure presented in our previous work,[12] and nano-scaled crystalline particles with diameter of ~10 nm (see Figure S4) were obtained. The electrodes were prepared by mixing the obtained Mn_3O_4 powders with Super-P carbon black (Imerys) and polyvinylidene difluoride (PVDF, Kynar, reagent grade) in a 8:1:1 weight ratio in the presence of N-methyl pyrrolidinone (NMP, Aldrich, >99%). Then, the electrode film was formed by tape casting the mixture slurry onto different current collectors (graphite foil (Gif), Cu foil (Cuf), Ni foil (Nif) and stainless steel foil (SSf)), followed by vacuum drying at 120 ºC for 10 hours. The dried film was punched into discs with 16 mm diameter and ~0.6 mg mass loading per disc. Coin cells (2016) with a Mg counter electrode (which was polished with SiC paper and cleaned before using) were used for the studies of the electrochemical performances of the synthesized Mn_3O_4 electrodes in APC electrolytes. The measurements of the galvanostatic charge/discharge were conducted using a Maccor 4200 (Maccor Inc., USA) battery analyzer at ambient temperature. By using the coin cell configuration, the electrochemical impedance spectra (EIS) were obtained on a Gamry Reference 600 instrument (Pennsylvania, USA) and fitted by using ZView software. The input AC perturbation was 5 mV, and the applied frequencies ranged from 0.01 Hz to 10 kHz. Cyclic voltammetry (CV) measurements of the Mn_3O_4 electrodes were carried out on the Gamry instrument by using a 3-electrode cell (EL-CELL), where the Mg metal served as both the reference electrode and the counter electrode.

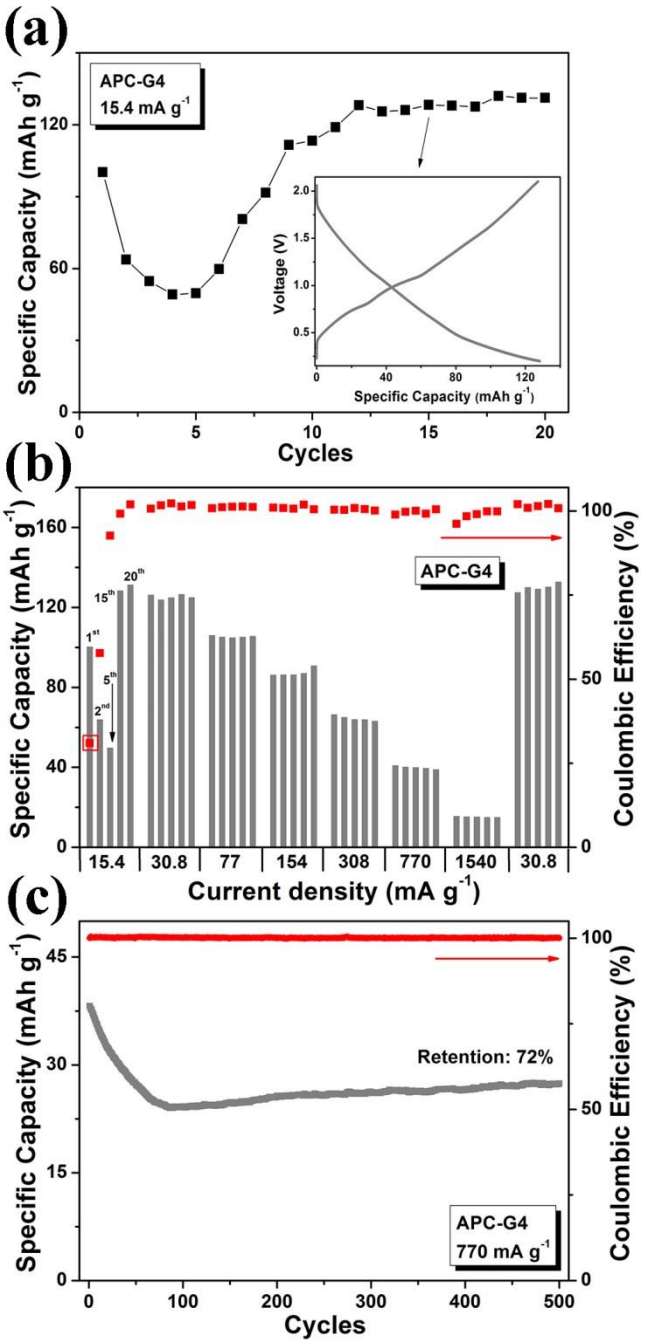

Figure S1. Electrochemical charge storage performance of the Mn_3O_4 cathode in APC-G4 electrolyte. (a) Cyclic stability at 15.4 mA g^{-1}. (b) Rate cyclic performance. (c) Long-term cycling at 770 mA g^{-1}. Inset: galvanostatic charge/discharge profiles at 15.4 mA g^{-1}.

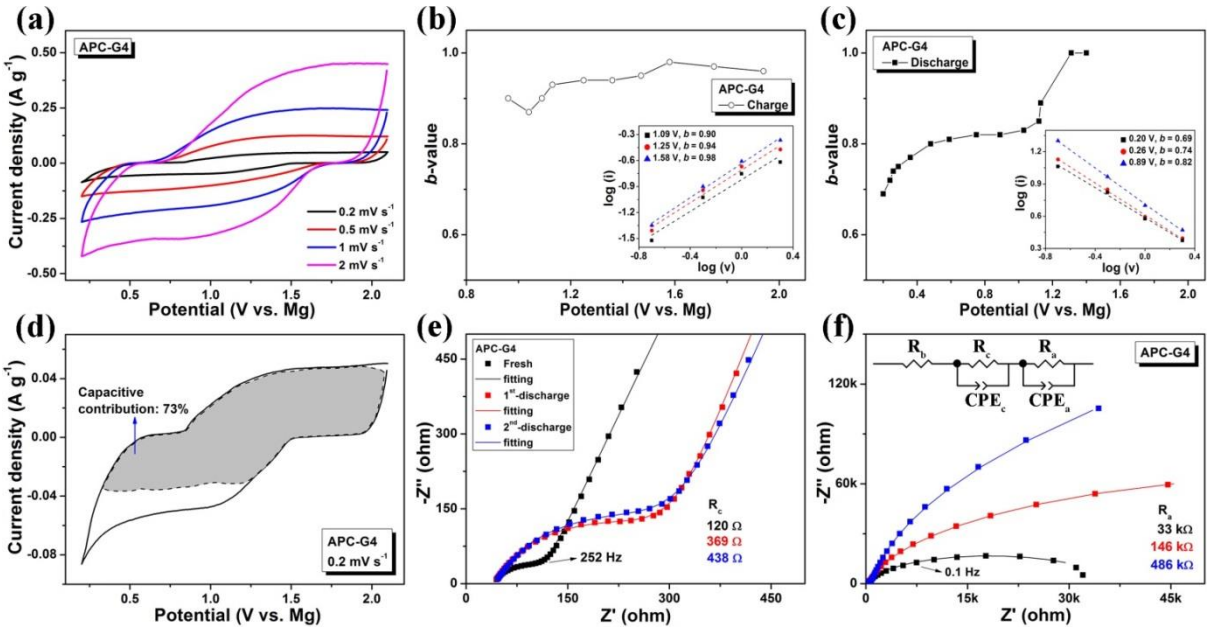

Figure S2. Kinetics, quantitative and impedance analysis of the Mn_3O_4 cathodes in APC-G4 electrolyte. (a) CV curves at different scan rates. Dependence of *b*-values as a function of potential for (b) anodic sweeps and (c) cathodic sweeps, respectively. Insets: power law dependence of current as a function of sweep rate. (d) The capacitive contribution (which corresponds to the shaded region, and determined from the data in Figure S3a) to the total stored charge at 0.2 mV s^{-1}. (e) The high frequency region and (f) the whole frequency region of the Nyquist plots of Mn_3O_4 electrodes at different cell states under 15.4 mA g^{-1}. Inset: the used equivalent circuits for data fitting.

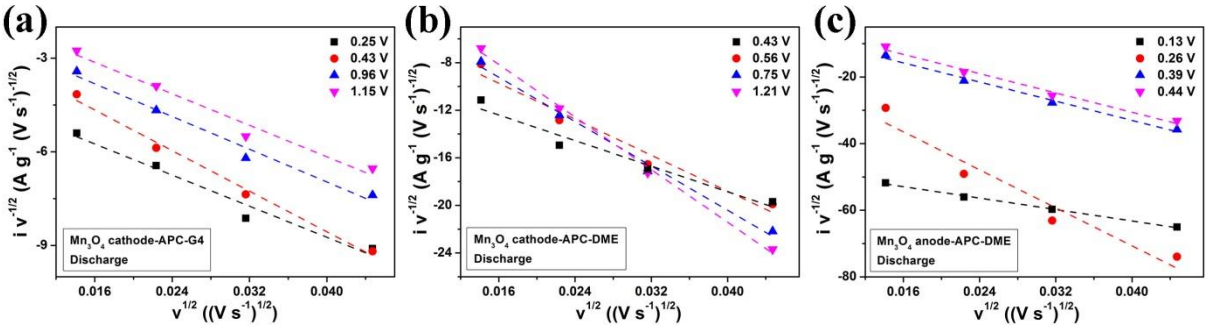

Figure S3. The plots of $v^{1/2}$ vs i $v^{-1/2}$. The scan rates are varied from 0.2 to 2 mV s^{-1}.

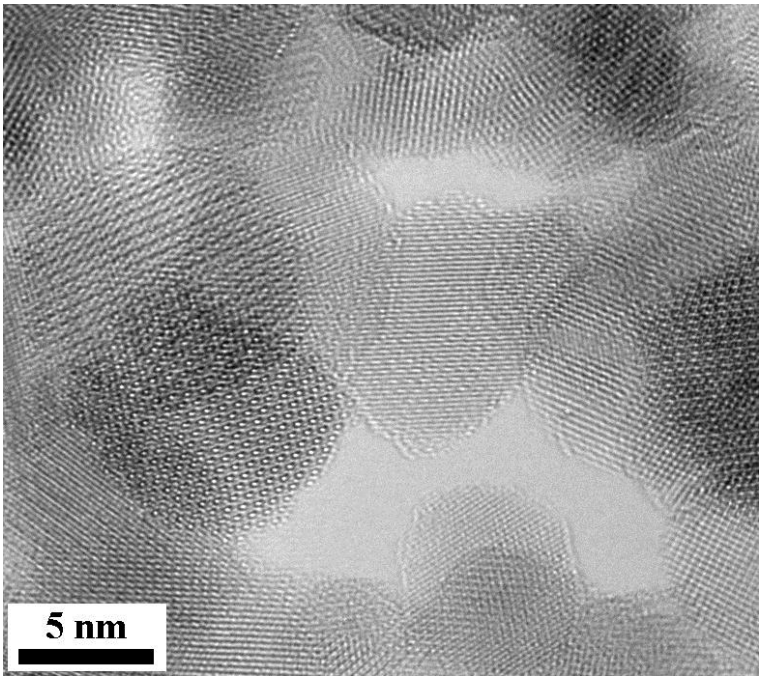

Figure S4. TEM image of the pristine Mn_3O_4 electrode.

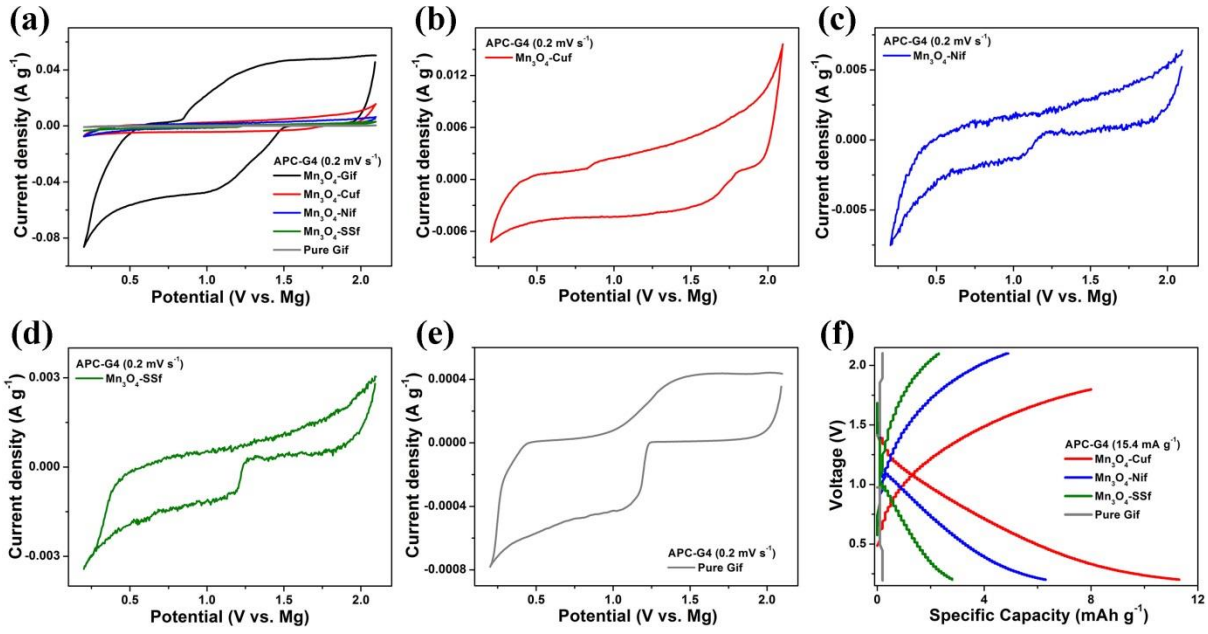

Figure S5. (a) Comparison of CV curves at 0.2 mV s^{-1} in APC-G4 electrolyte. CV curves of (b) Mn_3O_4-Cuf, (c) Mn_3O_4-Nif, (d) Mn_3O_4-SSf and (e) pure Gif at 0.2 mV s^{-1} in APC-G4 electrolyte. (e) Galvanostatic charge/discharge profiles at 15.4 mA g^{-1} in APC-G4 electrolyte.

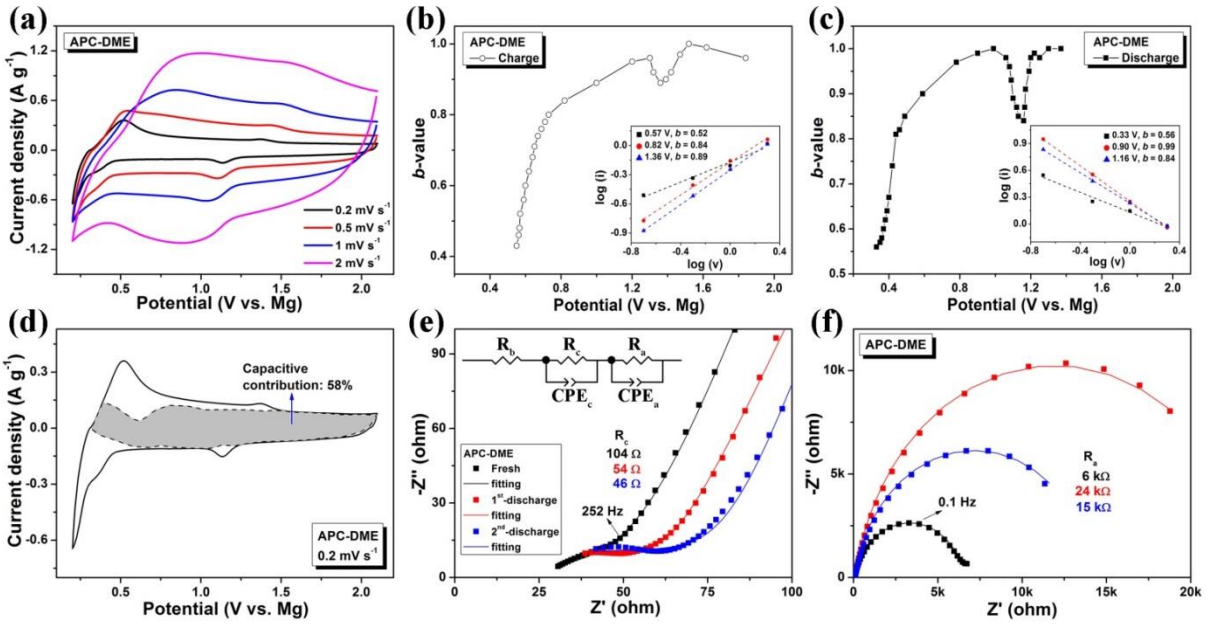

Figure S6. Kinetics, quantitative and impedance analysis of the Mn_3O_4 cathode in APC-DME electrolyte. (a) CV curves at different scan rates. Dependence of *b*-values as a function of potential for (b) anodic sweeps and (c) cathodic sweeps. Insets: power law dependence of current as a function of sweep rate. (d) The capacitive contribution (corresponding to the shaded region, and is determined from the data in Figure S3b) to the total stored charge at 0.2 mV s^{-1}. (e) The high-frequency region and (f) the whole frequency region of the Nyquist plots of the Mn_3O_4 electrodes at different cell states under 15.4 mA g^{-1}. Inset: equivalent circuits used for data fitting.

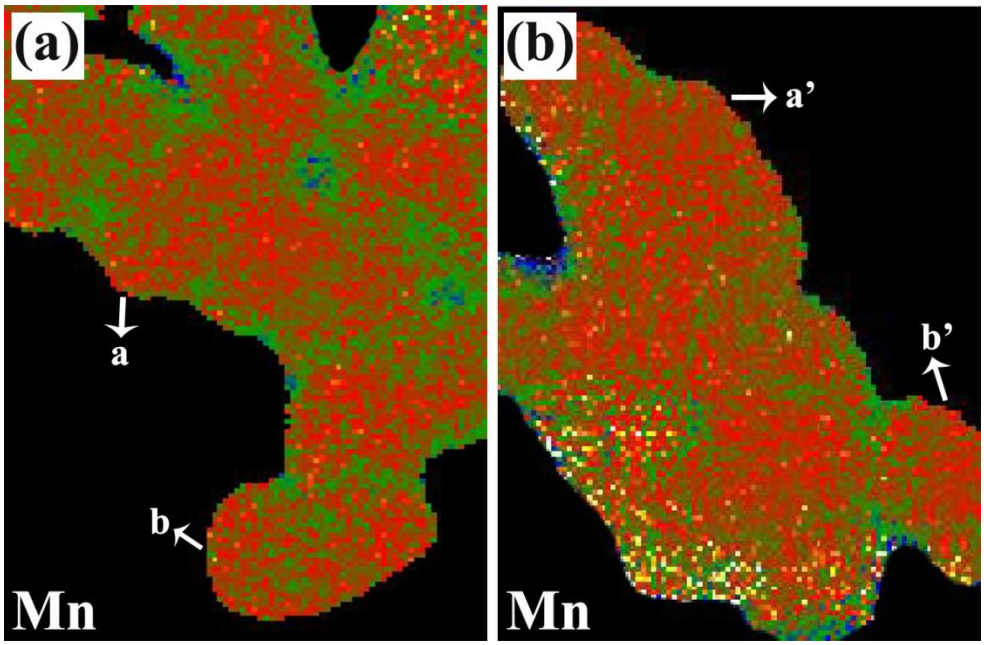

Figure S7. (a,b) The relative concentrations of Mn after quantification of EEL spectrum image that correspond to the STEM images shown in Figure 4a and 4d, respectively.

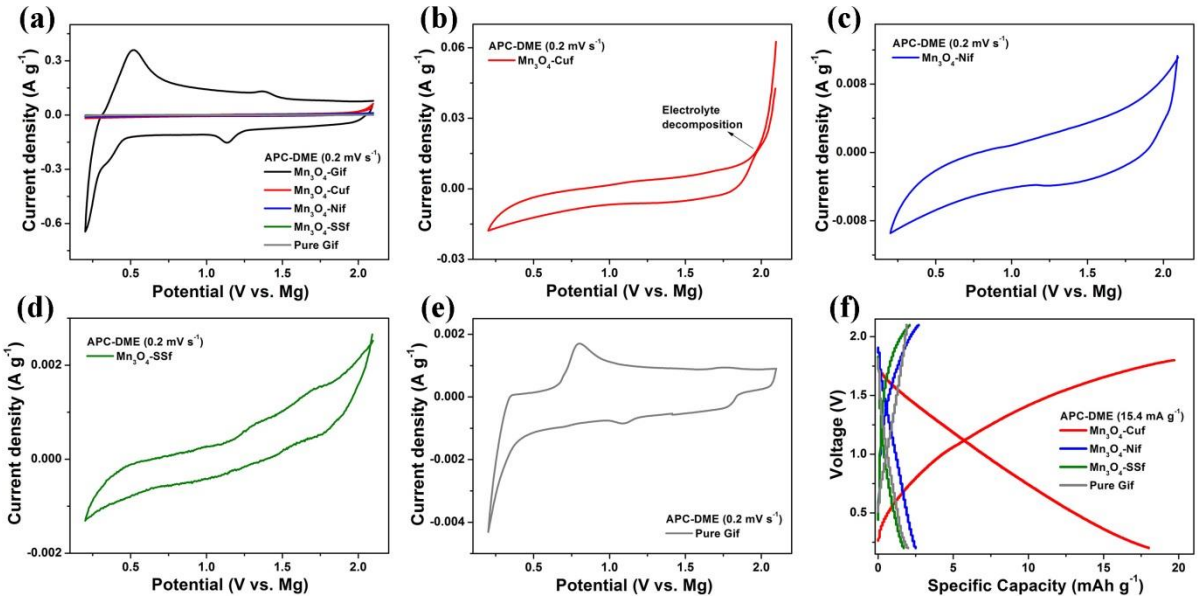

Figure S8. (a) Comparison of CV curves at 0.2 mV s^{-1} in APC-DME electrolyte. CV curves of (b) Mn_3O_4-Cuf, (c) Mn_3O_4-Nif, (d) Mn_3O_4-SSf and (e) pure Gif at 0.2 mV s^{-1} in APC-DME electrolyte. (e) Galvanostatic charge/discharge profiles at 15.4 mA g^{-1} in APC-DME electrolyte.

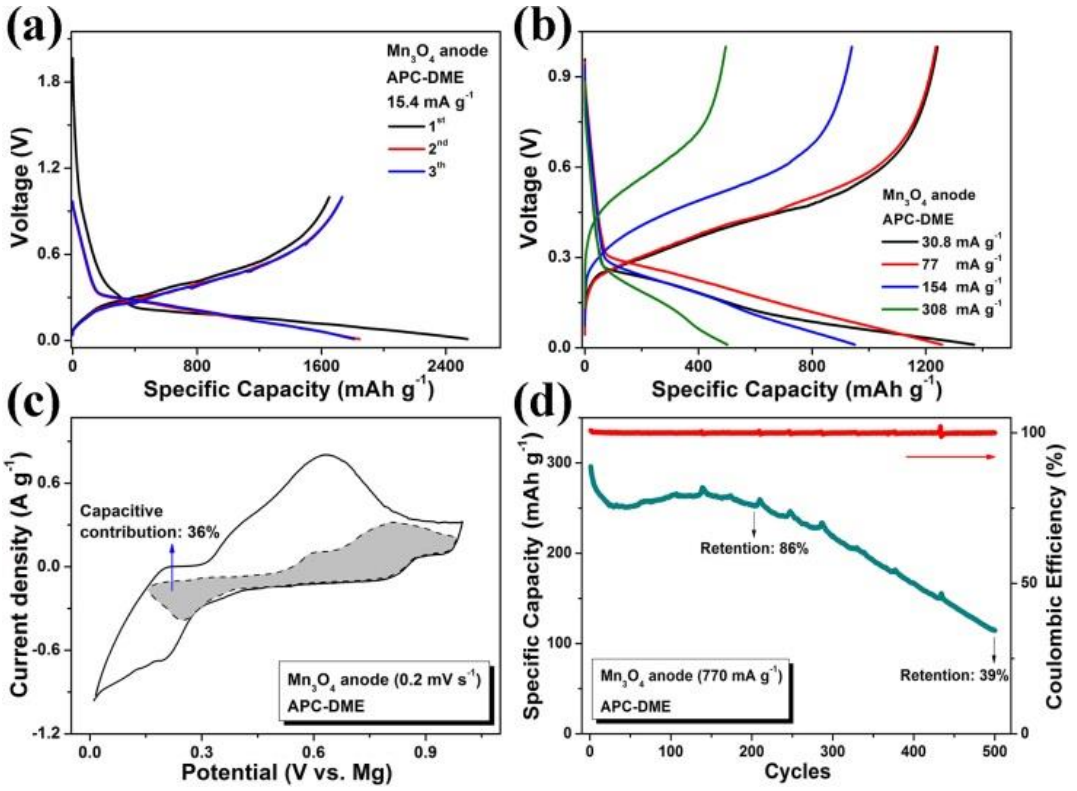

Figure S9. Electrochemical charge storage performance and quantitative analysis of the Mn_3O_4 anode in APC-DME electrolyte. (a,b) Galvanostatic charge/discharge profiles at different current densities. (c) The capacitive contribution (which corresponds to the shaded region, and determined from the data in Figure S3c) to the total stored charge at 0.2 mV s^{-1}. (d) Long cycle life at 770 mA g^{-1}.

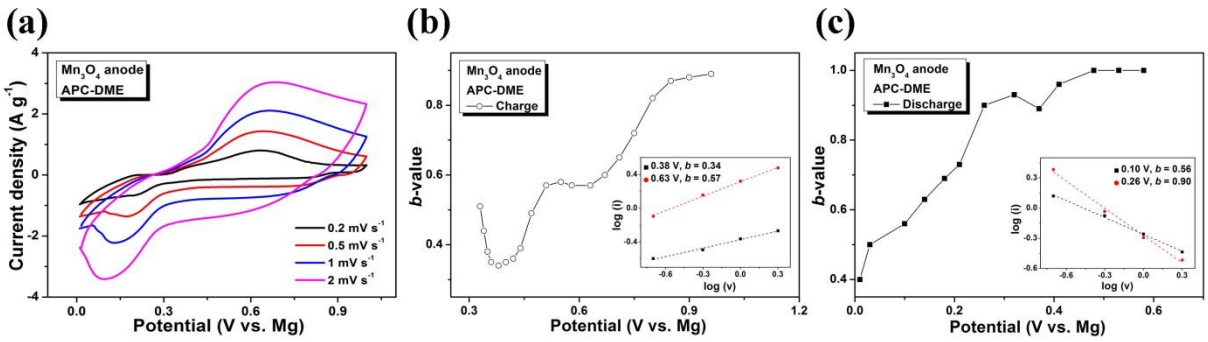

Figure S10. (a) CV curves of the Mn_3O_4 anode at different scan rates in APC-DME electrolyte. Dependence of *b*-values as a function of potential for (b) anodic sweeps and (c) cathodic sweeps. Insets show the power law dependence of current as a function of sweep rate.

Table S1 A survey of electrochemical performance of cathodes in Mg battery

Cathode materials	[a]Initial discharge capacity	Cycling stability	Rate capability	Ref (year)
		Metal oxides		
Mn_3O_4	790 mAh g^{-1} at 15.4 mA g^{-1}	100% after 500 cycles at 770 mA g^{-1}	70 mAh g^{-1} at 1.5 A g^{-1}	This work
MnO_2	~150 mAh g^{-1} at 500 mA g^{-1}	~33% after 160 cycles at 500 mA g^{-1}	-	13
MnO_2	~160 mAh g^{-1} at 985.6 mA g^{-1}	~67% after 200 cycles at 985.6 mA g^{-1}	-	14
α-MnO_2	~280 mAh g^{-1} at 36 μA cm^{-2}	~25% after 6 cycles at 36 μA cm^{-2}	-	15
λ-MnO_2	~330 mAh g^{-1} at 60 mA g^{-1}	57% after 5 cycles at 60 mA g^{-1}	-	16
Birnessite MnO_2	~230 mAh g^{-1} at 100 mA g^{-1}	~62% after 1000 cycles at 2 A g^{-1}	~100 mAh g^{-1} at 2 A g^{-1}	17
Mn_2O_4	150 mAh g^{-1} at 13.5 mA g^{-1}	-	-	18
V_2O_5	180 mAh g^{-1} at 0.15 mV s^{-1}	~83% after 15 cycles at 0.15 mV s^{-1}	-	19
V_2O_5	~220 mAh g^{-1} at 40 mA g^{-1}	~58% after 100 cycles at 320 mA g^{-1}	~100 mAh g^{-1} at 640 mA g^{-1}	20
$V_2O_5 \cdot nH_2O$	~25 mAh g^{-1} at 20 μA cm^{-2}	50 mAh g^{-1} after 10 cycles at 20 μA cm^{-2}	-	21
VO_x	218 mAh g^{-1} at 60 mA g^{-1}	~70% after 20 cycles at 60 mA g^{-1}	-	22

VO_x	124 mAh g^{-1} at 60 mA g^{-1}	50% after 80 cycles at 60 mA g^{-1}	-	23
V_2O_5/graphene	~320 mAh g^{-1} at 50 mA g^{-1}	~81% after 200 cycles at 1 A g^{-1}	100 mAh g^{-1} at 2 A g^{-1}	24
[b]GO/V_2O_5	178 mAh g^{-1} at 38.8 mA g^{-1}	~71% after 20 cycles at 38.8 mA g^{-1}	-	25
V_2O_5/CNF	~150 mAh g^{-1} at 20 mA g^{-1}	~125 mAh g^{-1} after 50 cycles at 37.5 mA g^{-1}	~100 mAh g^{-1} at 37.5 mA g^{-1}	26
V_2O_5-P_2O_5	121 mAh g^{-1} at 5 mA g^{-1}	~47% after 5 cycles at 5 mA g^{-1}	-	27
S-MnO_2-V_2O_5	~420 mAh g^{-1} at 60 mA g^{-1}	-	-	28
$FePO_4$	12 mAh g^{-1} at 20 μA cm^{-2}	~50% after 20 cycles at 20 μA cm^{-2}	-	29
MoO_3	210 mAh g^{-1} at 0.02 mV s^{-1}	~76% after 15 cycles at 0.02 mV s^{-1}	-	30
MoO_3	220 mAh g^{-1} at 0.3 mA cm^{-2}	~95% after 10 cycles at 0.3μA cm^{-2}	-	19
Co_3O_4	74 mAh g^{-1} at 0.1 mA	~60% after 30 cycles at 0.02 mA	-	31
RuO_2	101 mAh g^{-1} at 0.6 mA	~80% after 25 cycles at 0.6 mA	-	32
Ternary oxides				
$Mo_{2.48}VO_{9.93}$	397 mAh g^{-1} at 2 mA g^{-1}	100% after 25 cycles at 4 mA g^{-1}	114 mAh g^{-1} at 10 mA g^{-1}	33
$Ag_xMn_8O_{16}$	178 mAh g^{-1} at 50 mA g^{-1}	47% after 20 cycles at 50 mA g^{-1}	~15 mAh g^{-1} at 200 mA g^{-1}	34
$K_xMn_8O_{16}$	251 mAh g^{-1} at 50 mA g^{-1}	75% after 20 cycles at 50 mA g^{-1}	~50 mAh g^{-1} at 200 mA g^{-1}	34
$Mn_{2.15}Co_{0.37}O_4$	~60 mAh g^{-1} at 0.1 mA cm^{-2}	~50% after 30 cycles at 0.1 mA cm^{-2}	-	35
$Mg_{0.1}V_2O_5$	[d]~300 mAh g^{-1}	[d]~83% after 7 cycles	-	36
$Mg_{1.5}MnO_3$	~13 mAh g^{-1} at 7 mA g^{-1}	~100% after 19 cycles at 7 mA g^{-1}	-	37
$MgMn_2O_4$	220 mAh g^{-1} at 27 mA g^{-1}	28% after 40 cycles at 27 mA g^{-1}	110 mAh g^{-1} at 540 mA g^{-1}	38
Mg_xMnO_2 ·yH_2O	~220 mAh g^{-1} at 0.1 mA cm^{-2}	~45% after 20 cycles at 0.1 mA cm^{-2}	-	39

$Mg_{1.1}Mn_6O_{12}$ ·$4.5H_2O$	~250 mAh g^{-1} at 10 mA g^{-1}	~90% after 200 cycles at 100 mA g^{-1}	~20 mAh g^{-1} at 1 A g^{-1}	40
$Mg_{1.6}Mn_6O_{12}$ ·$5.7H_2O$	~300 mAh g^{-1} at 10 mA g^{-1}	~84% after 300 cycles at 100 mA g^{-1}	~25 mAh g^{-1} at 1 A g^{-1}	41
$Mg_xMo_{2.5+y}VO_{9+z}$	176 mAh g^{-1} at 2 mA g^{-1}	~57% after 30 cycles at 10 mA g^{-1}	~100 mAh g^{-1} at 20 mA g^{-1}	42
Mg silicates				
$Mg_{1.03}Mn_{0.97}SiO_4$	~115 mAh g^{-1} at 62.9 mA g^{-1}	~104% after 80 cycles at 62.9 mA g^{-1}	-	43
$MgFeSiO_4$	330 mAh g^{-1} at 6.62 mA g^{-1}	~100% after 5 cycles at 6.62 mA g^{-1}	-	44
$MgCoSiO_4$	~170 mAh g^{-1} at 30.57 mA g^{-1}	~128% after 15 cycles at 61.14 mA g^{-1}	~40 mAh g^{-1} at 183.42 mA g^{-1}	45
$Mg_{1.03}Mn_{0.97}SiO_4$	~210 mAh g^{-1} at 62.8 mA g^{-1}	~96% after 20 cycles at 62.8 mA g^{-1}	-	46
[e]MWNT/C/ $Mg_{1.03}Mn_{0.97}SiO_4$	~300 mAh g^{-1} at 62.9 mA g^{-1}	~100% after 23 cycles at 157.3 mA g^{-1}	~120 mAh g^{-1} at 157.3 mA g^{-1}	47
Sulfides				
CoS	~125 mAh g^{-1} at 50 mA g^{-1}	~85% after 60 cycles at 50 mA g^{-1}	~90 mAh g^{-1} at 150 mA g^{-1}	48
TiS_2	236 mAh g^{-1} at 10 mA g^{-1}	~78% after 80 cycles at 10 mA g^{-1}	140 mAh g^{-1} at 40 mA g^{-1}	49
Ti_2S_4	200 mAh g^{-1} at ~12 mA g^{-1}	-	190 mAh g^{-1} at ~47 mA g^{-1}	50
MoS_2	170 mAh g^{-1} at 20 mA g^{-1}	95% after 50 cycles at 20 mA g^{-1}	-	51
MoS_2/C	213 mAh g^{-1} at 50 mA g^{-1}	~39% after 50 cycles at 50 mA g^{-1}	-	52
MoS_2/RGO[f]	~105 mAh g^{-1} at 20 mA g^{-1}	~87% after 50 cycles at 20 mA g^{-1}	76 mAh g^{-1} at 50 mA g^{-1}	53
MoS_2/graphene	~116 mAh g^{-1} at 20 mA g^{-1}	~70% after 50 cycles at 20 mA g^{-1}	-	54
Mo_6S_8	~105 mAh g^{-1} at 15.25 mA g^{-1}	~90% after 100 cycles at 15.25 mA g^{-1}	-	55
Mo_6S_8	110 mAh g^{-1} at 15.25 mA g^{-1}	~95% after 250 cycles at 128 mA g^{-1}	80 mAh g^{-1} at 128 mA g^{-1}	56
$Cu_xMo_6S_8$	~125 mAh g^{-1} at 6 mA g^{-1}	~98% after 30 cycles at 12 mA g^{-1}	~90 mAh g^{-1} at 1.2 A g^{-1}	57

$Mg_xMo_3S_4$	~122 mAh g^{-1} at 0.3 mA cm^{-2}	~100% after 600 cycles at 0.3 mA cm^{-2}	-	58
$Mg_xMo_6S_6Se_2$	~110 mAh g^{-1} at 15.25 mA g^{-1}	~91% after 100 cycles at 15.25 mA g^{-1}	~80 mAh g^{-1} at 122 mA g^{-1}	59
Selenides				
WSe_2	~220 mAh g^{-1} at 50 mA g^{-1}	~92% after 160 cycles at 50 mA g^{-1}	103 mAh g^{-1} at 3 A g^{-1}	60
$TiSe_2$	~130 mAh g^{-1} at 5 mA g^{-1}	~69% after 50 cycles at 5 mA g^{-1}	103 mAh g^{-1} at 3 A g^{-1}	61
Cu_2Se	~260 mAh g^{-1} at 5 mA g^{-1}	~85% after 4 cycles at 5 mA g^{-1}	-	62
Carbon allotropes				
Fullerenes	50 mAh g^{-1} at 19 μA cm^{-2}	8% after 10 cycles at 75 μA cm^{-2}	22 mAh g^{-1} at 1.5 mA cm^{-2}	63
Fluorinated graphene	110 mAh g^{-1} at 10 mA g^{-1}	80% after 30 cycles at 100 mA g^{-1}	50 mAh g^{-1} at 100 mA g^{-1}	64
Graphite fluorides	813 mAh g^{-1} at 20 mA g^{-1}	-	430 mAh g^{-1} at 400 mA g^{-1}	65
Graphite fluorides	572 mAh g^{-1} at 10 mA g^{-1}	-	-	66
Organic-based cathodes				
1,4-polyanthraquinone	~130 mAh g^{-1} at 130 mA g^{-1}	~80% after 100 cycles at 130 mA g^{-1}	~50 mAh g^{-1} at 1.3 A g^{-1}	67
Poly(hydroquinoyl-benzoquinonyl sulfide)	~70 mAh g^{-1} at 50 mA g^{-1}	158 mAh g^{-1} after 20 cycles at 50 mA g^{-1}	-	68
2,5-Dimethoxy-1,4-Benzoquinone	226 mAh g^{-1} at 63.8 mA g^{-1}	~33 after 30 cycles at 63.8 mA g^{-1}	-	69
poly(antraquinoyl) sulfide	225 mAh g^{-1} at 50 mA g^{-1}	~22% after 100 cycles at 50 mA g^{-1}	~100 mAh g^{-1} at 500 mA g^{-1}	70
Others				
VOCl	170 mAh g^{-1} at 5 mA g^{-1}	~76% after 70 cycles at 5 mA g^{-1}	-	71
AgCl	178 mAh g^{-1} at 23 mA g^{-1}	~45% after 100 cycles at 930 mA g^{-1}	104 mAh g^{-1} at 1.86 A g^{-1}	72

[a] the value of the capacities were obtained at room temperature

[b] GO: graphite oxide. [c] CNF: carbon nanofoam. [d] current density not provided.

[e] MWNT: multiwalled carbon nanotubes. [f] RGO: reduced graphene oxide

Table S2 A survey of electrochemical performance of anodes in Mg battery

Anode materials	[a]Initial discharge capacity	Cycling stability	Rate capability	Ref (year)
Mn_3O_4	~2500 mAh g^{-1} at 15.4 mA g^{-1}	~86% after initial 200 cycles at 770 mA g^{-1}	~250 mAh g^{-1} at 770 mA g^{-1}	This work
MnO_2/AB[b]	310 mAh g^{-1} at 100 mA g^{-1}	~0% after 20 cycles at 100 mA g^{-1}	-	73
$MgMn_2O_4$	150 mAh g^{-1} at 60 μA	~60% after 20 cycles at 60 μA	-	74
Sn	~450 mAh g^{-1} at 4.5 mA g^{-1}	~51% after 10 cycles at 9 mA g^{-1}	~180 mAh g^{-1} at 45 mA g^{-1}	75
Sn	346 mAh g^{-1} at ~54 mA g^{-1}	90% after 30 cycles at ~135 mA g^{-1}	~290 mAh g^{-1} at ~135 mA g^{-1}	76
SnSb/graphene	~420 mAh g^{-1} at 50 mA g^{-1}	~80% after 200 cycles at 50 mA g^{-1}	-	77
Bi	350 mAh g^{-1} at 19.25 mA g^{-1}	~92% after 200 cycles at 19.25 mA g^{-1}	216 mAh g^{-1} at 1.9 A g^{-1}	78
Bi	~400 mAh g^{-1} at 192.5 mA g^{-1}	~50% after 100 cycles at 192.5 mA g^{-1}	-	79
TiS_2	270 mAh g^{-1} at ~12 mA g^{-1}	-	140 mAh g^{-1} at ~47 mA g^{-1}	80
$Li_4Ti_5O_{12}$	175 mAh g^{-1} at 15 mA g^{-1}	100% after 500 cycles at 300 mA g^{-1}	300 mAh g^{-1} at 50 mA g^{-1}	81
$Na_2Ti_3O_7$	~135 mAh g^{-1} at 20 mA g^{-1}	96% after 500 cycles at 200 mA g^{-1}	40 mAh g^{-1} at 1 A g^{-1}	82
Natural graphite	35 mAh g^{-1} at 37.2 mA g^{-1}	63% after 100 cycles at 37.2 mA g^{-1}	-	83

[a] the value of the capacities were obtained at room temperature.

[b] AB: acetylene black.

SUPPLEMENTARY REFERENCE

(1) Blöchl, P. E. *Phys. Rev. B* **1994**, *50*, 17953-17979.
(2) Kresse, G.; Hafner, J. *Phys. Rev. B* **1993**, *47*, 558-561.
(3) Kresse, G.; Hafner, J. *Phys. Rev. B* **1994**, *49*, 14251-14269.
(4) Kresse, G.; Furthmüller, J. *Comput. Mater. Sci.* **1996**, *6*, 15-50.
(5) Kresse, G.; Furthmuller, J. *Phys. Rev. B* **1996**, *54*, 11169-11186.
(6) Perdew, J. P.; Ruzsinszky, A.; Csonka, G. I.; Vydrov, O. A.; Scuseria, G. E.; Constantin, L. A.; Zhou, X.; Burke, K. *Phys. Rev. Lett.* **2008**, *100*, 136406-136406.
(7) Kresse, G.; Joubert, D. *Phys. Rev. B* **1999**, *59*, 1758-1775.
(8) Setyawan, W.; Gaume, R. M.; Lam, S.; Feigelson, R. S.; Curtarolo, S. *ACS Comb. Sci.* **2011**, *13*, 382-390.
(9) Henkelman, G.; Uberuaga, B. P.; Jónsson, H. *J. Chem. Phys.* **2000**, *113*, 9901-9904.
(10) Liu, M.; Rong, Z.; Malik, R.; Canepa, P.; Jain, A.; Ceder, G.; Persson, K. A. *Energy Environ. Sci.* **2015**, *8*, 964-974.
(11) Yoo, H. D.; Shterenberg, I.; Gofer, Y.; Gershinsky, G.; Pour, N.; Aurbach, D. *Energy Environ. Sci.* **2013**, *6*, 2265-2279.
(12) Wang, L.; Asheim, K.; Vullum, P. E.; Svensson, A. M.; Vullum-Bruer, F. *Chem. Mater.* **2016**, *28*, 6459-6470.
(13) Sun, X.; Duffort, V.; Mehdi, B. L.; Browning, N. D.; Nazar, L. F. *Chem. Mater.* **2016**, *28*, 534-542.
(14) Song, J.; Noked, M.; Gillette, E.; Duay, J.; Rubloff, G.; Lee, S. B. *Phys. Chem. Chem. Phys.* **2015**, *17*, 5256-5264.
(15) Zhang, R.; Yu, X.; Nam, K. W.; Ling, C.; Arthur, T. S.; Song, W.; Knapp, A. M.; Ehrlich, S. N.; Yang, X. Q.; Matsui, M. *Electrochem. Commun.* **2012**, *23*, 110-113.
(16) Kim, J. S.; Chang, W. S.; Kim, R. H.; Kim, D. Y.; Han, D. W.; Lee, K. H.; Lee, S. S.; Doo, S. G. *J. Power Sources* **2015**, *273*, 210-215.
(17) Nam, K. W.; Kim, S.; Lee, S.; Salama, M.; Shterenberg, I.; Gofer, Y.; Kim, J. S.; Yang, E.; Park, C. S.; Kim, J. S.; Lee, S. S.; Chang, W. S.; Doo, S. G.; Jo, Y. N.; Jung, Y.; Aurbach, D.; Choi, J. W. *Nano Lett.* **2015**, *15*, 4071-4079.
(18) Kim, C.; Phillips, P. J.; Key, B.; Yi, T.; Nordlund, D.; Yu, Y. S.; Bayliss, R. D.; Han, S. D.; He, M.; Zhang, Z.; Burrell, A. K.; Klie, R. F.; Cabana, J. *Adv. Mater.* **2015**, *27*, 3377-3384.
(19) Gershinsky, G.; Yoo, H. D.; Gofer, Y.; Aurbach, D. *Langmuir* **2013**, *29*, 10964-10972.
(20) Cheng, Y.; Shao, Y.; Raju, V.; Ji, X.; Mehdi, B. L.; Han, K. S.; Engelhard, M. H.; Li, G.; Browning, N. D.; Mueller, K. T.; Liu, J. *Adv. Funct. Mater.* **2016**, *26*, 3446-3453.
(21) Sa, N.; Kinnibrugh, T. L.; Wang, H.; Sai Gautam, G.; Chapman, K. W.; Vaughey, J. T.; Key, B.; Fister, T. T.; Freeland, J. W.; Proffit, D. L.; Chupas, P. J.; Ceder, G.; Bareno, J. G.; Bloom, I. D.; Burrell, A. K. *Chem. Mater.* **2016**, *28*, 2962-2969.
(22) Kim, R. H.; Kim, J. S.; Kim, H. J.; Chang, W. S.; Han, D. W.; Lee, S. S.; Doo, S. G. *J. Mater. Chem. A* **2014**, *2*, 20636-20641.
(23) Kim, J. S.; Kim, R. H.; Yun, D. J.; Lee, S. S.; Doo, S. G.; Kim, D. Y.; Kim, H. *ACS Appl. Mater. Interfaces* **2016**, *8*, 26657-26663.
(24) An, Q.; Li, Y.; Deog Yoo, H.; Chen, S.; Ru, Q.; Mai, L.; Yao, Y. *Nano Energy* **2015**, *18*, 265-272.
(25) Du, X.; Huang, G.; Qin, Y.; Wang, L. *RSC Adv.* **2015**, *5*, 76352-76355.
(26) Tepavcevic, S.; Liu, Y. Z.; Zhou, D. H.; Lai, B.; Maser, J.; Zuo, X. B.; Chan, H.; Kral, P.; Johnson, C. S.; Stamenkovic, V.; Markovic, N. M.; Rajh, T. *ACS Nano* **2015**, *9*, 8194-8205.
(27) Arthur, T. S.; Kato, K.; Germain, J.; Guo, J. H.; Glans, P. A.; Liu, Y. S.; Holmes, D.; Fan, X. D.; Mizuno, F. *Chem. Commun.* **2015**, *51*, 15657-15660.
(28) Inamoto, M.; Kurihara, H.; Yajima, T. *Materials* **2013**, *6*, 4514-4522.
(29) Zhang, R.; Ling, C. *ACS Appl. Mater. Interfaces* **2016**, *8*, 18018-18026.
(30) Spahr, M. E.; Novak, P.; Haas, O.; Nesper, R. *J. Power Sources* **1995**, *54*, 346-351.
(31) Sutto, T. E.; Duncan, T. T. *Electrochim. Acta* **2012**, *80*, 413-417.
(32) Sutto, T. E.; Duncan, T. T. *Electrochim. Acta* **2012**, *79*, 170-174.
(33) Kaveevivitchai, W.; Jacobson, A. J. *Chem. Mater.* **2016**, *28*, 4593-4601.
(34) Huang, J.; Poyraz, A. S.; Takeuchi, K. J.; Takeuchi, E. S.; Marschilok, A. C. *Chem. Commun.* **2016**, *52*, 4088-4091.
(35) Sanchez, L.; PereiraRamos, J. P. *J. Mater. Chem.* **1997**, *7*, 471-473.
(36) Lee, S. H.; DiLeo, R. A.; Marschilok, A. C.; Takeuchi, K. J.; Takeuchi, E. S. *ECS Electrochem. Lett.* **2014**, *3*, 87-90.
(37) Saha, P.; Jampani, P. H.; Hong, D.; Gattu, B.; Poston, J. A.; Manivannan, A.; Datta, M. K.; Kumta, P. N. *Mater. Sci. Eng., B* **2015**, *202*, 8-14.

(38) Yin, J.; Brady, A. B.; Takeuchi, E. S.; Marschilok, A. C.; Takeuchi, K. J. *Chem. Commun.* **2017**, *53*, 3665-3668.
(39) Kumagai, N.; Komaba, S.; Sakai, H.; Kumagai, N. *J. Power Sources* **2001**, *97*, 515-517.
(40) Zhang, H.; Ye, K.; Huang, X.; Wang, X.; Cheng, K.; Xiao, X.; Wang, G.; Cao, D. *J. Power Sources* **2017**, *338*, 136-144.
(41) Zhang, H.; Ye, K.; Shao, S.; Wang, X.; Cheng, K.; Xiao, X.; Wang, G.; Cao, D. *Electrochim. Acta* **2017**, *229*, 371-379.
(42) Kaveevivitchai, W.; Huq, A.; Manthiram, A. *J. Mater. Chem. A* **2017**, *5*, 2309-2318.
(43) Nuli, Y. N.; Yang, J.; Wang, J. L.; Li, Y. *J. Phys. Chem. C* **2009**, *113*, 12594-12597.
(44) Orikasa, Y.; Masese, T.; Koyama, Y.; Mori, T.; Hattori, M.; Yamamoto, K.; Okado, T.; Huang, Z. D.; Minato, T.; Tassel, C.; Kim, J.; Kobayashi, Y.; Abe, T.; Kageyama, H.; Uchimoto, Y. *Sci. Rep.* **2014**, *4*, 5622.
(45) Zheng, Y.; NuLi, Y.; Chen, Q.; Wang, Y.; Yang, J.; Wang, J. *Electrochim. Acta* **2012**, *66*, 75-81.
(46) NuLi, Y.; Yang, J.; Li, Y.; Wang, J. *Chem. Commun.* **2010**, *46*, 3794-3796.
(47) NuLi, Y.; Zheng, Y.; Wang, F.; Yang, J.; Minett, A. I.; Wang, J.; Chen, J. *Electrochem. Commun.* **2011**, *13*, 1143-1146.
(48) He, D.; Wu, D.; Gao, J.; Wu, X.; Zeng, X.; Ding, W. *J. Power Sources* **2015**, *294*, 643-649.
(49) Tao, Z. L.; Xu, L. N.; Gou, X. L.; Chen, J.; Yuan, H. T. *Chem. Commun.* **2004**, 2080-2081.
(50) Sun, X.; Bonnick, P.; Duffort, V.; Liu, M.; Rong, Z.; Persson, K. A.; Ceder, G.; Nazar, L. F. *Energy Environ. Sci.* **2016**, *9*, 2273-2277.
(51) Liang, Y. L.; Feng, R. J.; Yang, S. Q.; Ma, H.; Liang, J.; Chen, J. *Adv. Mater.* **2011**, *23*, 640-643.
(52) Liu, Y. C.; Jiao, L. F.; Wu, Q.; Du, J.; Zhao, Y. P.; Si, Y. C.; Wang, Y. J.; Yuan, H. T. *J. Mater. Chem. A* **2013**, *1*, 5822-5826.
(53) Liu, Y.; Jiao, L.; Wu, Q.; Zhao, Y.; Cao, K.; Liu, H.; Wang, Y.; Yuan, H. *Nanoscale* **2013**, *5*, 9562-9567.
(54) Liu, Y.; Fan, L. Z.; Jiao, L. *J. Power Sources* **2017**, *340*, 104-110.
(55) Lancry, E.; Levi, E.; Gofer, Y.; Levi, M. D.; Aurbach, D. *J. Solid State Electrochem.* **2005**, *9*, 259-266.
(56) Ha, J. H.; Adams, B.; Cho, J. H.; Duffort, V.; Kim, J. H.; Chung, K. Y.; Cho, B. W.; Nazar, L. F.; Oh, S. H. *J. Mater. Chem. A* **2016**, *4*, 7160-7164.
(57) Choi, S. H.; Kim, J. S.; Woo, S. G.; Cho, W.; Choi, S. Y.; Choi, J.; Lee, K. T.; Park, M. S.; Kim, Y. J. *ACS Appl. Mater. Interfaces* **2015**, *7*, 7016-7024.
(58) Aurbach, D.; Lu, Z.; Schechter, A.; Gofer, Y.; Gizbar, H.; Turgeman, R.; Cohen, Y.; Moshkovich, M.; Levi, E. *Nature* **2000**, *407*, 724-727.
(59) Aurbach, D.; Suresh, G. S.; Levi, E.; Mitelman, A.; Mizrahi, O.; Chusid, O.; Brunelli, M. *Adv. Mater.* **2007**, *19*, 4260-4267.
(60) Liu, B.; Luo, T.; Mu, G. Y.; Wang, X. F.; Chen, D.; Shen, G. Z. *ACS Nano* **2013**, *7*, 8051-8058.
(61) Gu, Y.; Katsura, Y.; Yoshino, T.; Takagi, H.; Taniguchi, K. *Sci. Rep.* **2015**, *5*, 12486.
(62) Tashiro, Y.; Taniguchi, K.; Miyasaka, H. *Electrochim. Acta* **2016**, *210*, 655-661.
(63) Zhang, R.; Mizuno, F.; Ling, C. *Chem. Commun.* **2015**, *51*, 1108-1111.
(64) Xie, J.; Li, C.; Cui, Z.; Guo, X. *Adv. Funct. Mater.* **2015**, *25*, 6519-6526.
(65) Miao, X.; Yang, J.; Pan, W.; Yuan, H.; Nuli, Y.; Hirano, S. I. *Electrochim. Acta* **2016**, *210*, 704-711.
(66) Giraudet, J.; Claves, D.; Guerin, K.; Dubois, M.; Houdayer, A.; Masin, F.; Hamwi, A. *J. Power Sources* **2007**, *173*, 592-598.
(67) Pan, B.; Huang, J.; Feng, Z.; Zeng, L.; He, M.; Zhang, L.; Vaughey, J. T.; Bedzyk, M. J.; Fenter, P.; Zhang, Z.; Burrell, A. K.; Liao, C. *Adv. Energy Mater.* **2016**, *6*, 1600140.
(68) Bitenc, J.; Pirnat, K.; Mali, G.; Novosel, B.; Randon Vitanova, A.; Dominko, R. *Electrochem. Commun.* **2016**, *69*, 1-5.
(69) Pan, B.; Zhou, D.; Huang, J.; Zhang, L.; Burrell, A. K.; Vaughey, J. T.; Zhang, Z.; Liao, C. *J. Electrochem. Soc.* **2016**, *163*, A580-A583.
(70) Bitenc, J.; Pirnat, K.; Bancic, T.; Gaberscek, M.; Genorio, B.; Randon-Vitanova, A.; Dominko, R. *Chemsuschem* **2015**, *8*, 4128-4132.
(71) Minella, C. B.; Gao, P.; Zhao-Karger, Z.; Mu, X.; Diemant, T.; Pfeifer, M.; Chakravadhanula, V. S. K.; Behm, R. J.; Fichtner, M. *ChemElectroChem* **2017**, *4*, 738-745.
(72) Zhang, R.; Ling, C.; Mizuno, F. *Chem. Commun.* **2015**, *51*, 1487-1490.
(73) Rasul, S.; Suzuki, S.; Yamaguchi, S.; Miyayama, M. *Electrochim. Acta* **2012**, *82*, 243-249.
(74) Cabello, M.; Alcántara, R.; Nacimiento, F.; Ortiz, G.; Lavela, P.; Tirado, J. L. *CrystEngComm* **2015**, *17*, 8728-8735.
(75) Singh, N.; Arthur, T. S.; Ling, C.; Matsui, M.; Mizuno, F. *Chem. Commun.* **2013**, *49*, 149-151.
(76) Nguyen, D. T.; Tran, X. M.; Kang, J.; Song, S. W. *ChemElectroChem* **2016**, *3*, 1813-1819.
(77) Parent, L. R.; Cheng, Y.; Sushko, P. V.; Shao, Y.; Liu, J.; Wang, C. M.; Browning, N. D. *Nano Lett.* **2015**, *15*, 1177-1182.

(78) Shao, Y.; Gu, M.; Li, X.; Nie, Z.; Zuo, P.; Li, G.; Liu, T.; Xiao, J.; Cheng, Y.; Wang, C.; Zhang, J. G.; Liu, J. *Nano Lett.* **2014**, *14*, 255-260.
(79) Liu, Z.; Lee, J.; Xiang, G.; Glass, H. F.; Keyzer, E. N.; Dutton, S. E.; Grey, C. P. *Chem. Commun.* **2017**, *53*, 743-746.
(80) Sun, X. Q.; Bonnick, P.; Nazar, L. F. *ACS Energy Lett.* **2016**, *1*, 297-301.
(81) Wu, N.; Lyu, Y. C.; Xiao, R. J.; Yu, X. Q.; Yin, Y. X.; Yang, X. Q.; Li, H.; Gu, L.; Guo, Y. G. *NPG Asia Mater.* **2014**, *6*.
(82) Chen, C.; Wang, J.; Zhao, Q.; Wang, Y.; Chen, J. *ACS Energy Lett.* **2016**, *1*, 1165-1172.
(83) God, C.; Bitschnau, B.; Kapper, K.; Lenardt, C.; Schmuck, M.; Mautner, F.; Koller, S. *RSC Adv.* **2017**, *7*, 14168-14175.